Mechanism of mRNA transport in the nucleus

Diana Y. Vargas*, Arjun Raj*†, Salvatore A. E. Marras*, Fred Russell Kramer*, and Sanjay Tyagi*‡

*Department of Molecular Genetics, Public Health Research Institute, 225 Warren Street, Newark, NJ 07103; and †Courant Institute of Mathematical Sciences, New York University, 251 Mercer Street, New York, NY 10012

Edited by Joseph G. Gall, Carnegie Institution of Washington, Baltimore, MD, and approved October 4, 2005 (received for review July 5, 2005)

The mechanism of transport of mRNA–protein (mRNP) complexes from transcription sites to nuclear pores has been the subject of many studies. Using molecular beacons to track single mRNA molecules in living cells, we have characterized the diffusion of mRNP complexes in the nucleus. The mRNP complexes move freely by Brownian diffusion at a rate that assures their dispersion throughout the nucleus before they exit into the cytoplasm, even when the transcription site is located near the nuclear periphery. The diffusion of mRNP complexes is restricted to the extranucleolar, interchromatin spaces. When mRNP complexes wander into dense chromatin, they tend to become stalled. Although the movement of mRNP complexes occurs without the expenditure of metabolic energy, ATP is required for the complexes to resume their motion after they become stalled. This finding provides an explanation for a number of observations in which mRNA transport appeared to be an enzymatically facilitated process.

gene expression | live cell imaging | mRNA export | nuclear viscosity

After mRNAs are synthesized, processed, and become associated with a number of different proteins at the transcription site, they are released into the nucleoplasm (1). The mechanism by which these large mRNA–protein (mRNP) complexes then move through dense nucleoplasm to reach the nuclear pores has been the subject of intense study and speculation (2, 3). Early workers proposed that mRNP complexes are transferred along a chain of receptors until they reach a nuclear pore, expending metabolic energy in the process (4). This solid-state transport model is supported by observations made in fixed nuclei that show some transcripts distributed along tracks that originate from the locus of the parent gene (5, 6). A second theory, called the "gene-gating" hypothesis, proposes that active genes are situated near the nuclear periphery and that mRNAs exit the nucleus through the nearest pores (7). This idea is supported by observations that certain mRNAs exit from one side of the nucleus (8) and that, in yeast, many transcriptionally active gene loci are located near the nuclear periphery (9). By contrast, a number of other studies have found that mRNP complexes move quite freely within the nucleus (10–16). This view is supported by studies of the distribution of newly synthesized Balbiani ring RNA in the salivary gland cells of insects (11), fluorescence recovery after photobleaching and fluorescence correlation spectroscopy studies of probes that bind to the poly(A) tails of mRNAs (12–15), and from single-particle analysis of mRNP complexes bound to GFP-linked proteins (16).

Although the latter studies found that mRNP complexes are able to diffuse within the nuclear matrix, there was a paradoxical active transport component to their motility, because both a reduction in temperature and ATP depletion curtailed the mobility of the complexes (14–16). To better understand the nature of mRNP mobility, we have developed a system of fluorogenic probes and mRNA constructs that allows us to track individual mRNA molecules as they are transcribed, move within the nucleus, exit from the nuclear pores, and spread throughout the cytoplasm. This system enables us to detect differences in the behavior of different molecules of the same mRNA species and to understand how different microenvironments in the nucleus influence the mobility of individual mRNP complexes.

Our probes are small, hairpin-shaped oligonucleotides called molecular beacons (17, 18) that possess an internally quenched fluorophore whose fluorescence is restored upon hybridization to a specific nucleic acid sequence. To obtain single-molecule sensitivity, we engineered a host cell line to express an mRNA possessing multiple molecular beacon binding sites. The binding of many molecular beacons to each mRNA molecule renders them so intensely fluorescent that individual mRNA molecules can be detected and tracked. We found that the rate of mRNP diffusion is so fast that mRNP complexes are dispersed throughout the nucleus soon after their synthesis and well before the onset of significant export into the cytoplasm. Our analyses of the trajectories of individual mRNA complexes show that their motion is restricted to the interchromatin spaces. Sometimes the moving mRNP complexes become stalled within high-density chromatin but later begin to move again. The switch from stationary to mobile behavior depends on ATP.

Materials and Methods

Host Cell Lines and Reporter Gene. A DNA fragment containing 96 head-to-tail tandem repeats of the 50-nt-long sequence 5′-CAGGAGTTGTGTTTGTGGACGAAGAGCACCAGCCAGCTGATCGACCTCGA-3′ was prepared as described by Robinett *et al.* (19) and inserted into the plasmid pTRE-d2EGFP (Clontech) by using its multiple cloning sites. The resulting plasmid, pTRE-GFP-96-mer, was used to transfect CHO cell line CHO-AA8-Tet-off (Clontech), which possesses a stably integrated gene for the tetracycline-controlled Tet-off transactivator. A geneticin G418-resistant clone (CHO-GFP-96-mer) that responded to 10 ng/ml doxycycline in the medium by turning off its fluorescence within 24 h was selected. To obtain cells expressing histone H2B-GFP, this cell line was transfected with plasmid pBOS-H2BGFP (BD Biosciences), and a clone that exhibited an intense GFP signal in the nuclei was isolated.

Cells were cultured in the α modification of Eagle's minimal essential medium (Sigma) supplemented with 10% TET-System-Approved FBS (Clontech). Imaging was performed in phenol red-free OptiMEM (Invitrogen). Cells used in the ATP-depletion studies were first incubated in glucose-free Dulbecco's modified Eagle's medium (Invitrogen) containing 10 mM sodium azide and 60 mM 2-deoxyglucose for 30 min and then imaged in OptiMEM containing the same inhibitors. After this treatment, the mitochondria in the cells could not be stained by rhodamine 123 (Sigma), confirming that the inhibitors were effective (14).

Molecular Beacons. The sequences of the molecular beacons were Cy3 or Alexa-594–5′-CUUCGUCCACAAACACAACUCCUGAAG-3′-Black Hole Quencher 2. The backbone of the molecular beacons was composed of 2′-*O*-methylribonucleotides.

Live Cell Imaging. Cells were maintained at 37°C on the microscope stage by controlled heating of the objective and the culture dish (Delta T4 open system, Bioptechs, Butler, PA). Molecular beacons were dissolved in water at a concentration of 2.5 ng/μl, and an $\approx$0.1-

Conflict of interest statement: No conflicts declared.

This paper was submitted directly (Track II) to the PNAS office.

Abbreviations: mRNP, mRNA–protein; MSD, mean square displacement.

‡To whom correspondence should be addressed. E-mail: sanjay@phri.org.

www.pnas.org/cgi/doi/10.1073/pnas.0505580102

to 1-fl solution was microinjected into each cell by using a FemtoJet microinjection apparatus (Brinkmann). An Axiovert 200M inverted fluorescence microscope (Zeiss), equipped with a ×100 oil-immersion objective, a CoolSNAP HQ camera (Photometrics, Pleasanton, CA) cooled to −30°C, and OPENLAB acquisition software (Improvision, Sheffield, U.K.) were used to acquire the images.

Synthetic RNA Transcripts and Their Hybrids with Molecular Beacons. We prepared a series of pGEM plasmids (Promega) containing 1, 2, 4, 8, 16, 32, or 64 tandem repeats of the sequence described above. In addition, we excised the gene encoding GFP-mRNA-96-mer from pTRE-GFP-96-mer and inserted it into plasmid pGEM, because that plasmid contains a bacteriophage T7 promoter. To produce RNA transcripts possessing a different number of repeats, these plasmids were linearized and used as templates for *in vitro* transcription by T7 RNA polymerase. The transcript containing 96 repeats possessed a GFP-mRNA sequence, whereas the other transcripts only possessed the repeat motifs. Hybrids were formed by incubating 20 ng of transcripts with 20 ng of molecular beacons in 10 μl of 10 mM Tris·HCl (pH 8.0) containing 1 mM $MgCl_2$ at 37°C for 60 min and were then injected into the cells.

Results

Reporter mRNA and Its Host Cell Line. To detect individual mRNP molecules, we constructed an mRNA that encodes GFP and has a "towed array" of 96 head-to-tail tandem repeats of a 50-nt-long molecular beacon target sequence, followed by a polyadenylation signal in its 3′ untranslated region (Fig. 1*A*). In preliminary *in vitro* experiments, we found that a 300-fold increase in the fluorescence intensity of the molecular beacon occurs upon its binding to the target sequence, and that all of the target sites in the mRNA were capable of binding to molecular beacons. The gene for this "GFP-mRNA-96-mer" was placed under the control of a promoter whose activity could be controlled by the inclusion of doxycycline in the culture medium (20) and stably integrated into the genome of a CHO cell line.

Fig. 1 *B* and *C* shows that these cells express GFP when doxycycline is absent from the culture medium and do not express GFP when it is present in the culture medium. Northern blot analysis showed that RNA transcripts containing the GFP sequence, a 4,800-nt-long multimeric sequence, and a poly(A) tail are produced by these cells when they are grown in the absence of doxycycline. The expression of GFP demonstrates that, despite the presence of the 96 molecular beacon target sequences, the mRNA can be processed, exported from the nucleus, and translated normally. To detect single molecules, we microinjected Cy3-labeled molecular beacons that were complementary to a portion of each of the repeated target sequences into cells grown in the absence of doxycycline and into cells grown in the presence of doxycycline and imaged the cells 15 min later. Discrete "particles" with an apparent diameter of 0.2–0.3 μm were detected in the cells expressing GFP but were not present in the cells that were not expressing GFP (Fig. 1 *D–F*). The number of particles present in each cell was proportional to the level of GFP expression seen in the cell.

Particles seen in the nuclei were brighter than particles seen in the cytoplasm. This phenomenon occurs due to the rapid sequestration of the molecular beacons into the nucleus after they are microinjected into the cytoplasm, which leaves little time for them to bind to targets in the cytoplasm (21). The nuclei of the cells not expressing GFP did not exhibit this particulate pattern; instead, a uniform background fluorescence of low intensity was observed (Fig. 1*E*). When molecular beacons possessing a probe sequence that was not complementary to any sequence in the cell were injected into the cells, both the cells that were expressing GFP and the cells that were not expressing GFP exhibited a uniform background fluorescence of low intensity.

When cells expressing GFP-mRNA-96-mer were injected with molecular beacons that were complementary to the target sequences in the mRNA and were then incubated for an additional hour, the intensely labeled nuclear particles migrated to the cytoplasm (Fig. 1*G*), indicating that the binding of molecular beacons to the mRNA does not prevent the export of mRNA from the nucleus to the cytoplasm. Because the mRNAs are exported and translated normally, we assume that they are bound to the usual set of proteins that escort mRNAs from the sites of transcription in the nucleus, through the nuclear pores, and into the cytoplasm (1).

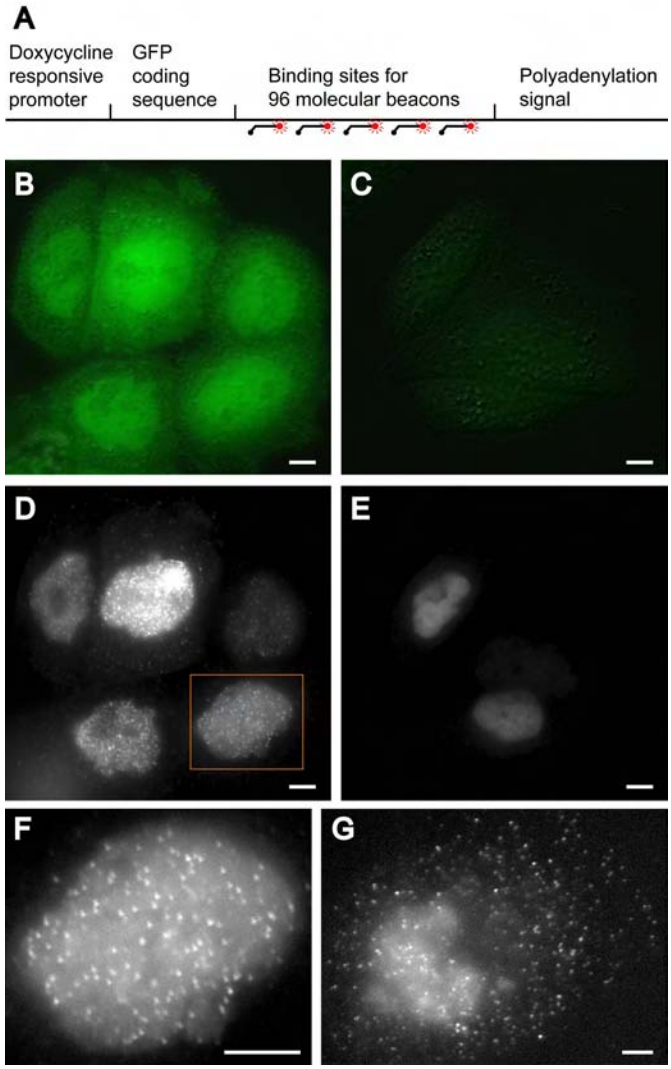

Fig. 1. Detection of individual mRNP particles in live cells. (*A*) Schematic representation of the structure of the engineered gene. Ninety-six copies of the same fluorescently labeled molecular beacon can simultaneously bind to the 3′ untranslated region of the mRNA (GFP-mRNA-96-mer) transcribed from this gene. (*B* and *C*) Images of live CHO cells possessing a stably integrated gene for GFP-mRNA-96-mer. An image of the cells' GFP fluorescence (green) is superimposed on a diffraction interference contrast image (gray scale). The cells shown in *B* were grown in the absence of doxycycline, enabling the expression of GFP-mRNA-96-mer, and the cells shown in *C* were grown in the presence of doxycycline, which suppresses the expression of the reporter mRNA. (*D* and *E*) Cy3 fluorescence images of the same group of cells as shown in *B* and *C*. A Cy3-labeled molecular beacon specific for the 96 tandemly repeated sequences present within the reporter mRNA was injected into the cells. (*F*) An enlargement of the nucleus, indicated by the box in *D*, showing individual fluorescently labeled mRNP particles. (*G*) A cell grown in the absence of doxycycline and imaged 1 h after the introduction of molecular beacons, showing the migration of mRNP particles from the nucleus to the cytoplasm. (Scale bars, 5 μm.)

CELL BIOLOGY

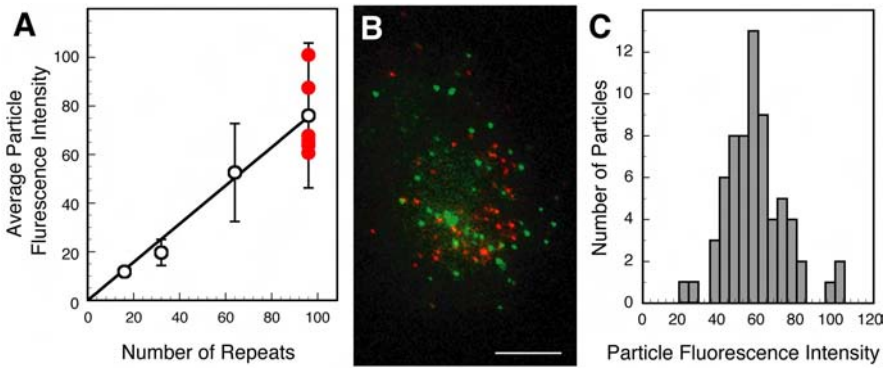

Fig. 2. Demonstration that each mRNP particle contains a single mRNA molecule. (*A*) Comparison of the fluorescence intensity of endogenous particles (red circles) to the fluorescence intensity of particles formed by the hybridization of molecular beacons to RNA transcripts that each possessed different numbers of molecular beacon binding sites (open circles). (*B*) Intracellular distribution of *in vitro*-transcribed GFP-96-mers hybridized to either Cy3-labeled molecular beacons that were specific for the repeated sequence (green) or to the same molecular beacons labeled with Alexa 594 (red). The hybrids were assembled separately *in vitro*, pooled, injected into the cytoplasm, and imaged with respect to each fluorophore. (*C*) Unimodal distribution of the fluorescence intensities of endogenous mRNP particles in a nucleus. (Scale bar, 5 μm.)

Demonstration That Each Particle Contains an Individual mRNA Molecule. Previous studies have shown that ≈48 GFP molecules, or 70 Cy3 moieties, can render a single molecular complex sufficiently fluorescent to enable its detection by using fluorescence microscopes similar to ours (16, 22). Thus, it is likely that single mRNA molecules hybridized to probes that aggregately contain 96 well dispersed Cy3 fluorophores would be similarly visible.

However, it is conceivable that the particles that we observed were produced by the multimerization of mRNAs or by the association of multiple mRNAs to structures present within the cell. To investigate this possibility, we prepared synthetic nucleic acid hybrids consisting of molecular beacons bound to *in vitro*-transcribed RNAs containing varying numbers of molecular beacon binding sites. These hybrids were then injected into CHO cells to compare their fluorescence intensity to the fluorescence intensity of the endogenously expressed mRNAs. Synthetic hybrids containing 96 binding sites produced particles with intensities roughly equal to the intensities displayed by the particles containing endogenous mRNA (Fig. 2*A*), indicating that the fluorescence of both types of particles arose from an equal number of molecular beacons. To be sure that particle intensity reflected the number of molecular beacons bound, we also measured the fluorescence intensity resulting from the injection of synthetic hybrids containing 16, 32, and 64 binding sites. The intensities of these particles were directly proportional to the number of binding sites, whereas RNAs possessing <16 binding sites did not produce detectable particles (Fig. 2*A*).

To show that the synthetic hybrids do not bind to each other and do not form multimers in association with cellular structures, *in vitro*-transcribed mRNAs possessing both a GFP-coding sequence and the 96-repeat motif were separately hybridized to two different molecular beacons possessing identical sequences but linked to different fluorophores. The two hybrid preparations were then mixed together and injected into CHO cells. When the cells were imaged with respect to each fluorophore, individual particles were found to be labeled with only one of the two fluorophores, and no particles were found to be labeled with both fluorophores (Fig. 2*B*).

Another line of evidence was obtained from a statistical analysis of the particle intensities. If the mRNA molecules have a tendency to aggregate in the cell, complexes of different sizes should occur, resulting in a multimodal distribution of particle intensities. However, when we measured the intensities of a large number of particles from the same nucleus, we found that their intensity distribution was unimodal (Fig. 2*C*). Finally, we found that the average number of mRNP particles per cell obtained from particle counting was similar to the average number of mRNA molecules per cell determined by real-time RT-PCR (Fig. 5, which is published as supporting information on the PNAS web site). Together, these results show that the endogenous mRNP particles observed in the cells each contain a single mRNA molecule.

mRNP Particles Explore the Volume of the Nucleus by Brownian Diffusion. In sequential images of the nucleus, the particles appear to move randomly within the nucleus (Movie 1, which is published as supporting information on the PNAS web site). About half of the nuclear particles were mobile, whereas the rest remained stationary during the 42-sec observation period. To explore the nature of their movements, we tracked individual particles as they moved within the nucleus (please see Table 2, which is published as supporting information on the PNAS web site, for the particle tracking method). The relationship between the mean square displacement (MSD) of a particle and the time interval between displacement measurements indicates whether the particles are diffusing freely, diffusing under constraints, such as tethers and walls, or are being carried by external agents, such as currents or molecular motors (23). A linear relationship between the observed MSD and the time interval signifies free diffusion, where the slope of the line is one-fourth of the diffusion constant when diffusion is observed in two dimensions (24). The majority of the moving particles (86%) displayed a linear relationship between MSD and the time interval (Fig. 3*A*), with the average value of their diffusion constant being 0.033 μm^2/sec.

For the rest of the moving particles, MSD increased linearly during short time intervals but reached a plateau during longer time intervals (Fig. 3*A*). The existence of this plateau suggests that the motion of these particles is confined to a cavity. The value of the square root of the maximum MSD is a measure of the radius of the constraining cavity, which was 0.5 μm on average. The particles diffuse freely within these cavities, as reflected by the linear increase of their MSD during short time periods (Fig. 3*A*). By comparison, measurements of stationary particles gave an average diffusion constant of only 0.0006 μm^2/sec (Fig. 3*A*), which is close to the lower limit of our ability to measure diffusion constants.

In comparison with the particles in the nucleus, almost all cytoplasmic particles were mobile. However, the average diffusion constant of the cytoplasmic particles (0.029 μm^2/sec) was similar. Occasionally, mRNP particles appeared to move by directed motion in the cytoplasm, which was never observed in the nucleus.

Dispersal of mRNP Particles from the Sites of Transcription. To study the kinetics of establishment of this steady-state distribution of mRNP particles, we imaged the dispersal of mRNP particles from the gene locus after induction of RNA synthesis. We first identified the gene locus by performing *in situ* hybridization in fixed cells with

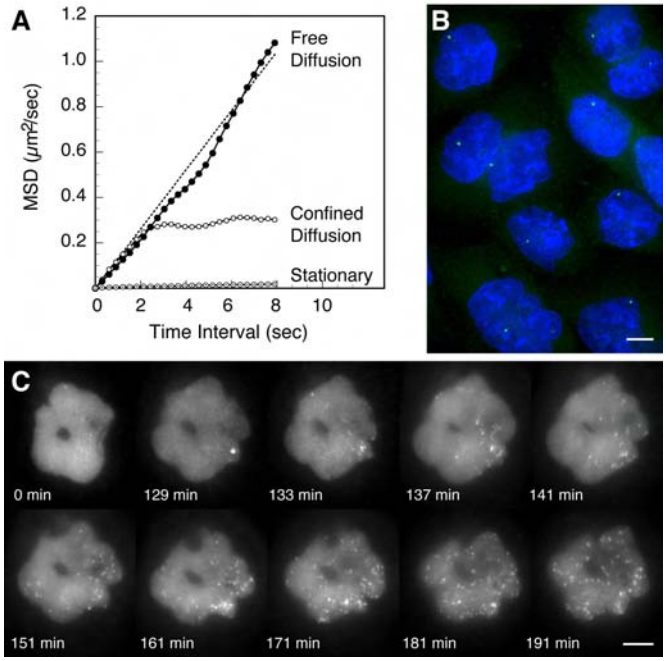

Fig. 3. Characterization of the diffusion of mRNP particles. (*A*) Relationship between the MSD of individual mRNP particles and the time interval during which the displacement occurred. Examples of three different types of behavior that were observed are shown. The dotted line indicates the results expected for freely diffusing particles with the average diffusion constant measured at 37°C. (*B*) Visualization of the locus of the gene that encodes the reporter mRNA. The image was obtained by *in situ* hybridization to cells whose DNA was denatured by heat and whose RNA was degraded by incubation with ribonuclease A by using a labeled oligonucleotide probe that is specific for the repeated sequence in the gene. The chromatin (stained with DAPI) is shown in blue, and the fluorescence of the probe is shown in green. (*C*) Dispersal of mRNP particles from the gene locus. Cells cultured in the presence of doxycycline to suppress the expression of the reporter mRNA were induced to express the reporter mRNA by the withdrawal of doxycycline while GFP-mRNA-96-mer was imaged. To view all of the particles, seven adjacent optical sections that were 0.2 μm apart were acquired for each time point and combined to form a single image. (Scale bars, 5 μm.)

oligonucleotide probes that were specific for the repeated sequence under conditions in which the cellular DNA was denatured and RNA was removed. Fig. 3*B* shows that a single site corresponding to the reporter gene is present in each nucleus and is located close to the nuclear envelope.

To image the dispersal of mRNA molecules from this gene locus, we cultured the cells in the presence of doxycycline, introduced the molecular beacons, and then removed doxycycline from the growth medium while continuously imaging the cells. Fig. 3*C* shows selected sequential images of a representative nucleus from a series of images that began immediately after induction. RNA synthesis occurred at a distinct site in the nucleus. The fluorescence intensity at this site was substantially higher than the usual intensity of individual mRNP particles, indicating the presence of a tightly organized cluster of multiple mRNA molecules at the locus. The RNA cluster usually became visible 60–90 min after induction. These mRNA clusters were relatively immobile (apparent diffusion constant <0.0006 μm^2/sec) compared with the rapid rate of diffusion of individual mRNP particles. The mRNA clusters were always present at the edge of a dense chromatin region. These chromatin-associated, immobile clusters of mRNA probably comprise nascent transcripts that are still attached to the gene via RNA polymerase, having not yet undergone the 3′-terminal processing events required for their release (10, 25).

As we continued to monitor the immobile cluster of nascent mRNA molecules, individual mRNA molecules emanating from the site dispersed isotropically throughout the nucleus (Fig. 3*C*). After ≈3 h, the mRNA molecules were fully dispersed in the nucleus with a slight crowding near the site of transcription, a pattern often seen in steadily expressing cells. Even though the gene locus was situated near the periphery of the nucleus, mRNP complexes were distributed uniformly within the nuclear volume before the onset of export into the cytoplasm.

Regions of the Nucleus That Permit Free Diffusion. Further analysis of mRNP mobility showed that some regions of the nucleus are inaccessible to mRNP particles. Time-lapse fluorescence images superimposed on diffraction interference contrast images suggested that mRNP particles do not enter the nucleoli. To confirm these observations, we stained the nucleoli using an antibody directed against the nucleolar protein fibrillarin (26) and detected individual mRNP particles by *in situ* hybridization. The resulting images (Fig. 4*A*) demonstrate that the mRNP particles remain outside the nucleoli.

To explore other impediments to the freedom of movement of mRNP particles, we studied their mobility in relation to chromatin density. We visualized chromatin density in the CHO cells by expressing a heterologous histone H2B fused to GFP. Histone H2B-GFP is incorporated into chromatin without substantially affecting cellular physiology, and its fluorescence intensity in different regions of the nucleus reflects the density of the chromatin in those regions (27). This visualization was possible, despite the simultaneous expression of GFP from the reporter RNA, because these GFP molecules yielded lower fluorescence intensity and did not concentrate in the nucleus.

We analyzed the motion of mRNP particles relative to the density of chromatin by two different methods. For nuclei possessing only a few particles, we tracked each mRNP particle and then superimposed the tracks on images of the chromatin density within the nuclei. The results revealed that the motion of the particles is restricted to regions where chromatin density is low, whereas immobile particles are embedded within regions where chromatin density is high (Fig. 4*B* and Movie 2, which is published as supporting information on the PNAS web site). Often, the tracks of mobile particles mirror the shape of the low-density chromatin cavities, channels, and saddle points.

For nuclei possessing many mRNP particles, we used a graphical method to distinguish regions frequently visited by mobile particles from regions where stationary particles rest. To locate the stationary particles, the images were averaged over the entire time series. This operation enhanced the apparent fluorescence intensity of the stationary particles, because they remain in the same small area over a large number of frames. However, the apparent fluorescence intensity of the mobile particles was attenuated in the averaged images because the particles move about, distributing their signal over a large area. To locate the regions in which the mobile mRNP particles travel, we subtracted the fluorescence intensity of every pixel in each frame from the fluorescence intensity of the corresponding pixel in the frame that was taken 4 sec earlier. In the resulting time series of difference images, only the new locations of the mobile particles were visible. We then merged all of the difference images into one composite image that highlighted the regions of the nucleus through which the particles traveled. The result is shown in Fig. 4*C*, in which chromatin is colored blue, stationary particles are colored red, and the space through which the mobile particles move is colored green. In addition, we used the series of difference images to prepare Movie 3, which is published as supporting information on the PNAS web site. The results of this analysis confirm that mRNP particles travel within chromatin-poor regions, and that the locations of stationary particles coincide with regions occupied by high-density chromatin.

On average, about half of the mRNP particles were mobile at any moment. Sometimes moving particles were seen to come to a stop,

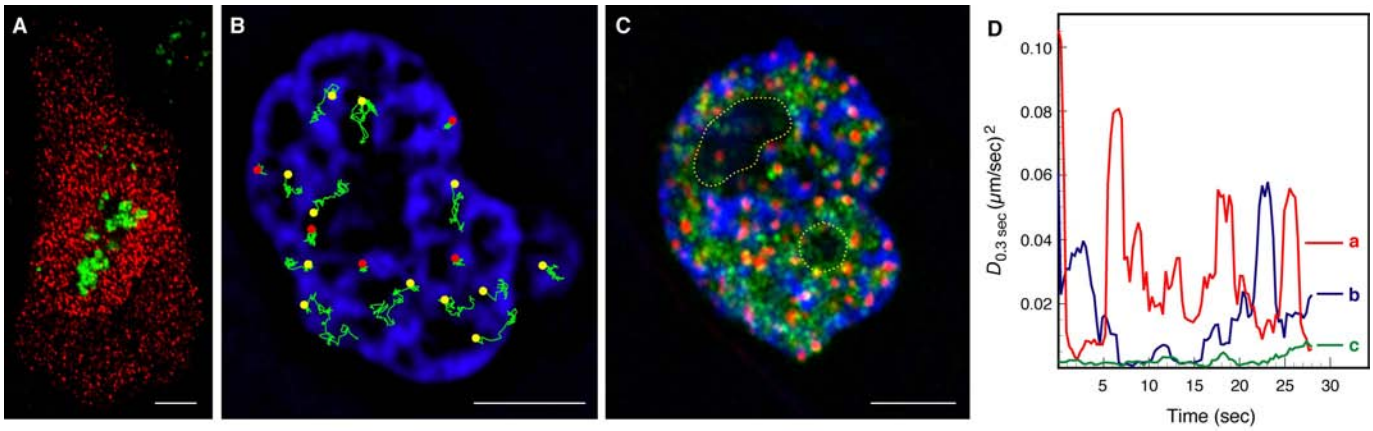

Fig. 4. Identification of the nuclear domains accessible to mRNP particles. (*A*) Distribution of mRNP particles around the nucleoli. The mRNP particles (red) were imaged by *in situ* hybridization with a labeled oligonucleotide that was complementary to the repeated sequence in GFP-mRNA-96-mer, and the nucleoli (green) were imaged by using a labeled antibody specific for the nucleolar protein fibrillarin. (*B*) Tracks of a few of the mRNP molecules in a nucleus overlaid on an image of chromatin density. The chromatin (blue) was visualized by the expression of a stably integrated gene for histone H2B that was fused with GFP. The image was obtained by deconvolution from nine optical sections that were 0.2 μm apart. The tracks of the particles classified as mobile terminate in a yellow dot, and the tracks of particles classified as stationary terminate in a red dot. (*C*) Regions frequently visited by mRNP particles determined from a graphical analysis of the motion of particles during 42 sec of observation. Regions occupied by stationary particles are shown in red, regions visited by mobile particles are shown in green, and the location of the chromatin is shown in blue. Dotted lines locate the boundaries of two nucleoli that were visible under diffraction interference contrast. (*D*) Change in the diffusion constant as a function of time for (*a*) a continuously moving mRNP particle; (*b*) for a particle that stalls (from 7 to 16 sec) and then begins to move again; and (*c*) for a stationary particle. The diffusion constants were measured for the 0.3-sec time interval between successive frames and averaged over a 1.5-sec-wide moving window. (Scale bars, 5 μm.)

sometimes stopped particles were seen to resume their motion, and sometimes the same particle was seen to stop for a short while and then move again (Fig. 4*D*). However, so few events of this type occurred during the time scale of our tracking experiments (45 sec) that it is difficult to quantify the time scale during which the stationary particles became mobile and vice versa. Because the stationary particles were usually found within regions of high-density chromatin, we can postulate that an mRNP particle can become trapped if it enters a small cavity surrounded by dense chromatin.

Effect of Low Temperature and ATP Depletion on the Mobility of mRNP Particles. To investigate the possible role of active transport in the movement of mRNP particles, we studied how their mobility is affected by a reduction in temperature (from 37°C to 25°C) and by a reduction in cellular ATP levels. To decrease the cellular ATP concentration, we incubated the cells in a glucose-free medium that contained 2-deoxyglucose, which is a glycolysis inhibitor, and sodium azide, which is an electron transport chain inhibitor (16, 28, 29). To characterize the mobility of the mRNP particles under these conditions, we measured their diffusion constants and determined the fraction of stalled and mobile particles.

When the temperature was reduced by 12°C, there was a 45% reduction in the average diffusion constant of the particles (Table 1 and Movie 4, which is published as supporting information on the PNAS web site). If the motion of the particles was due to Brownian diffusion, we would have expected only a 4% reduction because diffusion is directly proportional to absolute temperature when other physical conditions are held constant. *A priori*, this drop suggests that active processes control the movements of mRNP particles. However, upon ATP depletion, we found that the average diffusion constant of the mobile particles was identical to the average diffusion constant measured under physiological conditions (Table 1 and Movie 5, which is published as supporting information on the PNAS web site), suggesting that the motion of the mobile particles is not controlled by enzymatic processes.

This apparent contradiction could be resolved if lowering the temperature results in a large increase in the viscosity of the nucleoplasm, causing the observed drop in the diffusion constant of the mRNP particles. To explore this possibility, we microinjected a synthetic 64-mer RNA transcript that was hybridized to molecular beacons along its entire length. This construct could be similarly tracked but was unlikely to be actively transported because it did not have a coding sequence, 5′ cap, or poly(A) tail and was not produced *in situ*, so it was unlikely to couple with mRNA-binding proteins, which are conditions necessary for the assembly of functional mRNP complexes (1). To further reduce the likelihood that this synthetic hybrid would bind to mRNA-binding proteins during the course of the experiment, we initiated time-lapse imaging within 30 sec of its microinjection into the nucleus. Consistent with their smaller size and our hypothesis that mRNA-associated proteins do not bind to them, the diffusion constant of the synthetic hybrid

Table 1. Average diffusion constants and mobile fractions of mRNA particles

	Diffusion constant, μm^2/sec			Fraction of mobile particles, %		
RNA	37°C	25°C	−ATP, 37°C	37°C	25°C	−ATP, 37°C
Endogenous nuclear	0.033	0.018	0.034	53	33	26
Synthetic nuclear	0.061	0.043	0.043	72	43	52
Endogenous cytoplasmic	0.029	0.021	0.035			
Synthetic cytoplasmic	0.096	0.033	0.087			

For each category, we analyzed an average of 15 tracks distributed among 6 cells, with each track persisting for an average of 55 frames and no track persisting for <20 frames. SDs and additional data are presented in Table 2.

molecules was twice that of the endogenous mRNP particles under physiological conditions. Upon reduction of the temperature, the synthetic hybrids displayed a drop in diffusion constant that was similar in magnitude to the drop in the diffusion constant of the endogenous mRNP particles (Table 1). Because the synthetic transcripts were unlikely to be involved in enzymatic transport processes, these results suggest that the observed decrease in the average diffusion constant of the endogenous mRNP particles at lower temperatures is due to an increase in viscosity, rather than to the involvement of an active process.

Both the reduction in temperature and the depletion of ATP doubled the proportion of stalled mRNP particles (Table 1). When the temperature was returned to 37°C or the level of ATP was restored (Movie 5), the proportion of stalled particles returned to its normal level. Assuming a dynamic equilibrium between the mobile and the stalled states of the mRNP particles, this observation suggests that the rescue of particles from the stalled state to the mobile state is an ATP-dependent process.

Discussion

Earlier studies of the mobility of mRNA populations by using poly(A)-specific reporters led to seemingly contradictory conclusions that, although mRNP complexes move by diffusion, their mobility is curtailed upon depletion of ATP from the cell (14, 15). Both our observations that mRNP particles tend to get stalled when passing through high-density chromatin and that, upon ATP depletion, this tendency is accentuated, resulting in a larger population of stalled particles, help to resolve this contradiction. One possible explanation is that some constituents of mRNP complexes tend to bind to chromatin and that ATP is required to disrupt these bonds. A second possibility, which we favor more, is that ATP depletion alters the chromatin structure in such a way that a larger number of mRNP particles become stalled. What kinds of structural changes in chromatin may be able to bring this about? A relevant observation is that the flexibility of chromatin is decreased upon ATP depletion (30). Therefore, we postulate that high chromatin flexibility enables the frequent escape of mRNP particles from their corralled or stalled states. Thus, ATP depletion will result in an increase in the fraction of stalled particles without affecting the diffusion constant of mobile particles. Along similar lines, Shav-Tal and colleagues (16) have suggested that ATP depletion results in reduced "pore size" in the chromatin "mesh," which reduces the overall mobility of mRNP particles. Their view is supported by observations of reversible curdling in chromatin upon ATP depletion (16, 31).

The underlying concern that prompted the formulation of the solid-state active transport hypothesis (4, 5) and the gene-gating hypothesis (7) was that interphase nuclei are likely to be so viscous that large mRNP particles will not be able to diffuse freely within them. However, our analysis of the movements of individual mRNP particles shows that the nucleus possesses at least two distinct microenvironments: dense chromatin, within which mRNP particles do not move, and interchromatin spaces, within which the particles move as freely as they move in the cytoplasm. Other investigations that have explored the viscosity of nuclei support this conclusion. When fluorescently labeled high-molecular-weight dextrans are injected into nuclei, they distribute themselves throughout the interchromatin space and are excluded from dense areas of chromatin (32). Fluorescence recovery after photobleaching measurements of the diffusion constants of these dextrans indicate that the viscosity within the interchromatin spaces is similar to the viscosity of the cytoplasm (33). Furthermore, single-particle tracking of microspheres of 100 nm in diameter injected into nuclei reveals the presence of two separate phases in the nucleus: interstitial spaces of low viscosity that permit free diffusion, and other spaces of very high viscosity in which the microspheres are unable to move freely (34).

In all of the methods previously used to study the dynamics of mRNP complexes, the probes fluoresced whether they were bound to the target, were bound nonspecifically to other molecules, or were floating freely in the nucleoplasm. By comparison, the molecular beacon probes are nonfluorescent until they bind to their mRNA targets. Because we tracked discrete mRNP particles that contain a single mRNA target molecule, background fluorescence generated by the nonspecific association of molecular beacons with other molecules in the nucleus was uniformly distributed and had no influence on our analysis.

We have described an effective method for the detection and tracking of individual mRNA molecules in living cells. Natural genes can be engineered to have multiple molecular beacon target sites to study the mechanism of their transport in different cell types. This method will also be useful for the identification of cellular sites where other processes central to gene expression take place. Examples of such processes are mRNA splicing, maturation, export, decay, and localization. The ability to track multiple mRNAs tagged with different multimeric target sequences by using differently colored molecular beacons in the same cell will be especially useful in this regard.

We thank Diana Bratu, Musa M. Mhlanga, Charles S. Peskin, and Ben Gold for discussions. This work was supported by National Institutes of Health Grants GM-070357 and EB-000277.

1. Dreyfuss, G., Kim, V. N. & Kataoka, N. (2002) *Nat. Rev. Mol. Cell Biol.* **3,** 195–205.
2. Politz, J. C. & Pederson, T. (2000) *J. Struct. Biol.* **129,** 252–257.
3. Carmo-Fonseca, M., Platani, M. & Swedlow, J. R. (2002) *Trends Cell Biol.* **12,** 491–495.
4. Agutter, P. S. (1994) *Cell Biol. Int.* **18,** 849–858.
5. Lawrence, J. B., Singer, R. H. & Marselle, L. M. (1989) *Cell* **57,** 493–502.
6. Bridger, J. M., Kalla, C., Wodrich, H., Weitz, S., King, J. A., Khazaie, K., Krausslich, H. G. & Lichter, P. (2005) *Exp. Cell Res.* **302,** 180–193.
7. Blobel, G. (1985) *Proc. Natl. Acad. Sci. USA* **82,** 8527–8529.
8. Colon-Ramos, D. A., Salisbury, J. L., Sanders, M. A., Shenoy, S. M., Singer, R. H. & Garcia-Blanco, M. A. (2003) *Dev. Cell* **4,** 941–952.
9. Casolari, J. M., Brown, C. R., Komili, S., West, J., Hieronymus, H. & Silver, P. A. (2004) *Cell* **117,** 427–439.
10. Zachar, Z., Kramer, J., Mims, I. P. & Bingham, P. M. (1993) *J. Cell Biol.* **121,** 729–742.
11. Singh, O. P., Bjorkroth, B., Masich, S., Wieslander, L. & Daneholt, B. (1999) *Exp. Cell Res.* **251,** 135–146.
12. Politz, J. C., Browne, E. S., Wolf, D. E. & Pederson, T. (1998) *Proc. Natl. Acad. Sci. USA* **95,** 6043–6048.
13. Politz, J. C., Tuft, R. A., Pederson, T. & Singer, R. H. (1999) *Curr. Biol.* **9,** 285–291.
14. Calapez, A., Pereira, H. M., Calado, A., Braga, J., Rino, J., Carvalho, C., Tavanez, J. P., Wahle, E., Rosa, A. C. & Carmo-Fonseca, M. (2002) *J. Cell Biol.* **159,** 795–805.
15. Molenaar, C., Abdulle, A., Gena, A., Tanke, H. J. & Dirks, R. W. (2004) *J. Cell Biol.* **165,** 191–202.
16. Shav-Tal, Y., Darzacq, X., Shenoy, S. M., Fusco, D., Janicki, S. M., Spector, D. L. & Singer, R. H. (2004) *Science* **304,** 1797–1800.
17. Tyagi, S. & Kramer, F. R. (1996) *Nat. Biotechnol.* **14,** 303–308.
18. Bratu, D. P., Cha, B. J., Mhlanga, M. M., Kramer, F. R. & Tyagi, S. (2003) *Proc. Natl. Acad. Sci. USA* **100,** 13308–13313.
19. Robinett, C. C., Straight, A., Li, G., Willhelm, C., Sudlow, G., Murray, A. & Belmont, A. S. (1996) *J. Cell Biol.* **135,** 1685–1700.
20. Gossen, M. & Bujard, H. (1992) *Proc. Natl. Acad. Sci. USA* **89,** 5547–5551.
21. Tyagi, S. & Alsmadi, O. (2004) *Biophys. J.* **87,** 4153–4162.
22. Babcock, H. P., Chen, C. & Zhuang, X. (2004) *Biophys. J.* **87,** 2749–2758.
23. Saxton, M. J. & Jacobson, K. (1997) *Annu. Rev. Biophys. Biomol. Struct.* **26,** 373–399.
24. Berg, H. C. (1983) *Random Walks in Biology* (Princeton Univ. Press, Princeton).
25. Shatkin, A. J. & Manley, J. L. (2000) *Nat. Struct. Biol.* **7,** 838–842.
26. Kill, I. R. (1996) *J. Cell Sci.* **109,** 1253–1263.
27. Kanda, T., Sullivan, K. F. & Wahl, G. M. (1998) *Curr. Biol.* **8,** 377–385.
28. Wagner, S., Chiosea, S., Ivshina, M. & Nickerson, J. A. (2004) *J. Cell Biol.* **164,** 843–850.
29. Platani, M., Goldberg, I., Lamond, A. I. & Swedlow, J. R. (2002) *Nat. Cell Biol.* **4,** 502–508.
30. Heun, P., Laroche, T., Shimada, K., Furrer, P. & Gasser, S. M. (2001) *Science* **294,** 2181–2186.
31. Gorisch, S. M., Wachsmuth, M., Ittrich, C., Bacher, C. P., Rippe, K. & Lichter, P. (2004) *Proc. Natl. Acad. Sci. USA* **101,** 13221–13226.
32. Verschure, P. J., van der Kraan, I., Manders, E. M., Hoogstraten, D., Houtsmuller, A. B. & van Driel, R. (2003) *EMBO Rep.* **4,** 861–866.
33. Lukacs, G. L., Haggie, P., Seksek, O., Lechardeur, D., Freedman, N. & Verkman, A. S. (2000) *J. Biol. Chem.* **275,** 1625–1629.
34. Tseng, Y., Lee, J. S. H., Kole, T. P., Jiang, I. & Wirtz, D. (2004) *J. Cell Sci.* **117,** 2159–2167.